Lattice Dilation of Plasma Sprayed Nickel Film Quantified by High Resolution Terahertz Imaging

Anis Rahman[1]*, Francis Tanzella[2], Aunik K Rahman[1], Carl Page[3] and Robert Godes[4]

[1]Applied Research & Photonics, USA

[2]Energy Research Center LLC, USA

[3]Anthropocene Institute, USA

[4]Brillouin Energy, USA

Abstract

Lattice dilation of metallic nickel film deposited by plasma-spraying on a ceramic layer that is also prepared by plasma-spraying, has been investigated by high resolution terahertz imaging and sequential zooming of the images to quantify the lattice parameter by graphical analysis. A metallic nickel sample was first imaged, and its measured lattice constant was found to be in agreement with the known value. Subsequently, four additional samples containing plasma-sprayed nickel film have also been imaged via an identical procedure. The lattice images of all samples were used for graphical analysis and quantification of the respective lattice parameters. Four samples, viz., 77, 81, 129 and 111 have been analyzed and their lattice dilation was investigated. It was found that the lattice distance (d) of these samples is in the order as, $d_{77} < d_{81} < d_{129} < d_{111}$ and higher than the value of metallic nickel. Unit cell volume and density were also calculated for each sample from the measured lattice parameter. The density was found in the decreasing order for the 4 samples; i.e., $\rho_{77} > \rho_{81} > \rho_{129} > \rho_{111}$ and the density values are significantly lower than the value for nickel. To our knowledge, this is the first direct evidence of the lattice dilation of plasma-sprayed metallic nickel measured via the terahertz lattice imaging, without requiring an electron microscope. Thus, the results presented herein establish an exciting extension of camera-less, reconstructive terahertz imaging technique that produces such a clear lattice image of nickel and allows to quantify the lattice parameter. The technique, however, is a general one, applicable to any material.

Introduction

Lattice dilation is the root cause of many physical transformation of solid materials, including hydrogen embrittlement, crystal to glass transition, or in general, the amorphization of metals. This solid state amorphization can be induced by various perturbations. Such external stimuli include particle beam irradiations, chemical reactions, external electric field stress, and mechanical deformations. The signature of such amorphization is not easy to detect until some macroscopic change is manifested in a given structure. Therefore, a lattice scale direct evidence of such transition via lattice dilation is important for an early stage detection; such detection is not easy from SEM/TEM images because of the strictly 2D nature of those images. The unit cell of nickel is a face-centered cube with the lattice parameter of 0.352nm, giving an atomic radius of 0.124nm. This crystal structure is stable to pressures of at least 70 GPa. Nickel belongs to the transition metals; it is hard and ductile. In this paper, the lattice of metallic nickel has been investigated under different experimental conditions via terahertz high-resolution imaging technique [1]. The objectives of these investigations are to use the high-resolution images of the samples of the present study, known as the "Hydrogen Hot Tube (HHT)" or the LENR tube cells [2,3] as shown in Figure 1. As described in ref. [2], these HHTs are used for Iso Peri Bolic calorimeter experiments for investigating the low energy nuclear reaction (LENR) possibilities (see the Discussion section). It is hoped that the high-resolution images will shed light for understanding the mechanism via which the LENR effect, if any, may take place. However, the present investigation is also important for understanding the hydrogen embrittlement phenomenon [4] that occurs via lattice dilation.
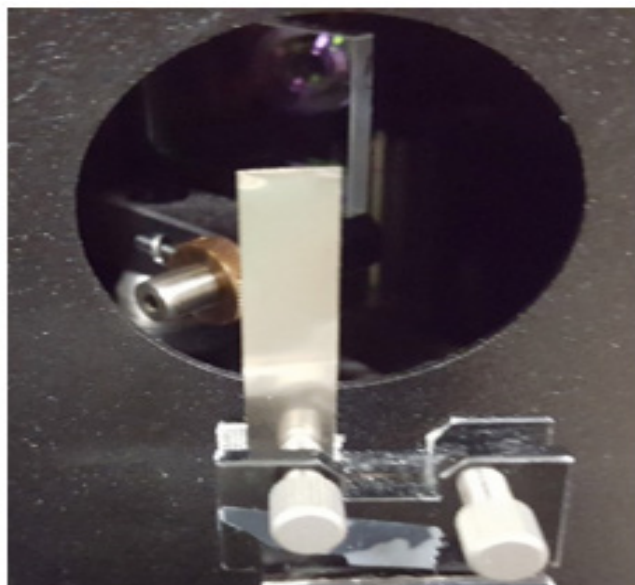
Figure 1: A strip of metallic nickel is mounted on the nano scanner.

In what follows, we first briefly review the camera-less lattice resolution imaging technique with terahertz wavelength [5-7]. Then we apply the imaging protocol on a metallic nickel sample to measure its lattice parameter. After that, we proceed with the characterization of the four LENR tube cells, as described in the experimental section. We then discuss the implications of the present findings in the context of a broader LENR related aspects in the light of key publications in the contemporary literature, following a few concluding remarks and future outlook.

Camera-less lattice scale imaging with terahertz waves

It is well known that the resolution of images those are formed by a focusing lens on a recording medium (photographic film or the Charged Coupled Device (CCD)), is determined by the Abbe Diffraction Limit (ADL) [8] that sets the resolution to the highest value of half the wavelength of the light used for imaging. It was recently demonstrated that the ADL may be overcome, and higher resolution images may be formed by terahertz multispectral reconstructive imaging [1]. Tt was further demonstrated that the combination of terahertz imaging and terahertz time-domain spectrometry can be used as a powerful tool for investigating semiconductor wafers, epitaxial layers, and nanomaterials [5-7]. Since most materials are transparent to the T-rays, terahertz imaging technique offers an important feature that the sub-surfaces may be probed and visualized in a non-destructive, non-contact fashion. This technique also offers another advantage for user definable pixel size (or voxel size in 3D) by a hardware and software combination; while a digital camera displays and records the processed signal of an object with fixed pixel size. In a camera, an object is focused on a CCD or a focal plane array by means of a focusing lens, the output of the CCD is processed by a built-in processor that displays the image on a screen and saves the image in a file. In contrast, the terahertz technique eliminates the CCD and lens system by using a nano scanner and a suitable computer algorithm for image generation and processing. Thus, the terahertz route eliminates the focusing lens and the CCD. Here, the object to be imaged is scanned (digitized) along the 3 orthogonal axes for 3D imaging; or digitized on a plane for surface imaging. A matrix containing the digitized reflected signal (or, equivalently, the transmitted signal) is recorded in a file and then processed by a suitable algorithm. The concept and the procedure for 3D image formation is described in detail elsewhere [1].

Experimental

Metallic nickel lattice

Terahertz imaging of the samples were carried out by a terahertz nanoscanning spectrometer and 3D imager (TNS3DI, Applied Research & Photonics, Harrisburg, PA). A metallic nickel strip was mounted on the nanoscanner as shown in Figure 1. The front-end software of the TNS3DI was used for automated positioning of the T-ray beam on the sample. Then the built-in software was used for rasterizing a small spot ($5\mu m \times 5\mu m \times 2\ \mu m$) of the sample. While nickel as metal is highly reflective, however, the TNS3DI's terahertz beam is able to penetrate $\sim 5\mu m$ thick aluminum foil; hence it is safe to image up to $2\mu m$ deep. The resulting reflected intensity matrix was used for subsequent image generation and analysis. Figure 2 & 3 exhibit the lattice image of the metallic nickel sample. A grey-scale profile of a few lattice planes is shown in Figure 4; this profile plot was used to measure the lattice parameter of nickel by the standard procedure of full width of half maximum (FWHM). The public domain software, Image J [9] was utilized for the quantitative measurements. The lattice parameter thus measured was 0.353nm which is the accepted value of the lattice constant of Face-Centered Cubic (FCC) nickel in bulk [10].
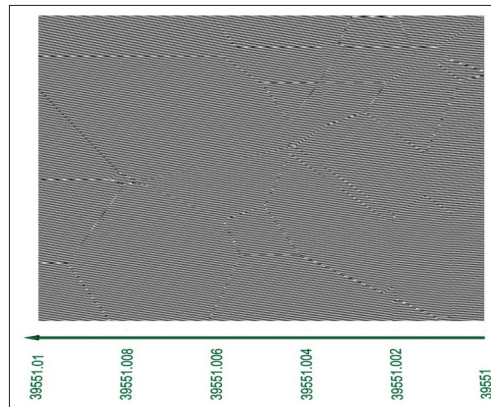
Figure 2: Lattice image of Nickel (in units of μm). Nanograins and boundaries are visible.
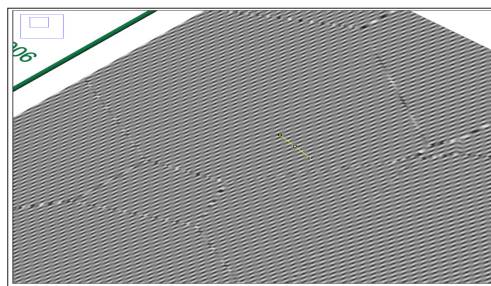

Figure 3: Lattice image of Nickel, same as Figure 2 but rotated and enlarged for lattice parameter calculation by graphical analysis.
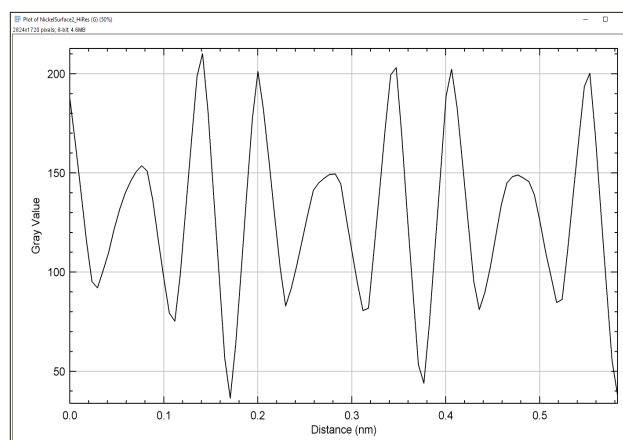

Figure 4: Graphical analysis of Figure 3 across the cursor. The measured lattice parameter of nickel is 0.353Å.

LENR tube cells

Four tubular LENR cells were received from Brillouin Energy [11]. The as received samples are named as 77, 81, 129 and 111. All samples were made by sequential plasma-spraying of respective layers on an alumina substrate which is a hardened alumina tube with ~6.35mm outer diameter. On to the alumina tube, a copper layer was first deposited by plasma-spraying technique. Subsequently, another layer of alumina was deposited on top of the copper layer see (Figure 5). Finally, a layer of nickel was also deposited on top of the alumina layer. Each coating layers were baked (annealed) before depositing the next layers as needed.

Sample 77 is the reference; that is, it is the as manufactured sample, without any further energy stress experiment. Sample 81 and 129 were stressed by a high energy RF electric field while heated at a higher temperature [12]. These two samples reportedly produced higher output energy than that applied as input. Also, sample 129 produced higher energy than sample 81 under identical experimental conditions. Sample 111 was also subjected to high input filed similar to the samples 81 and 129 but did not produce as much output energy as the others.

For terahertz imaging measurements, all samples were polished at a steep oblique angle for exposing the different constituent

layers, viz., the Cu, the ceramic and the nickel layers; as shown in Figure 5. Since the objective is to investigate the morphology and lattice condition of the nickel layer due to alumina interaction; therefore, imaging was carried out at a place in the nickel layer at the Ni-ceramic interface.

All samples were mounted one at a time on the nano scanner with the help of a special fixture (Figure 5). The nano scanner was manipulated by the built-in front-end software on all three orthogonal axes to pinpoint an area that is rich in nickel but located near the ceramic layer; i.e., near the nickel-ceramic interface. A course image scan was conducted on a 250µm × 250µm area following a finer scan over a volume up to 2µm deep.
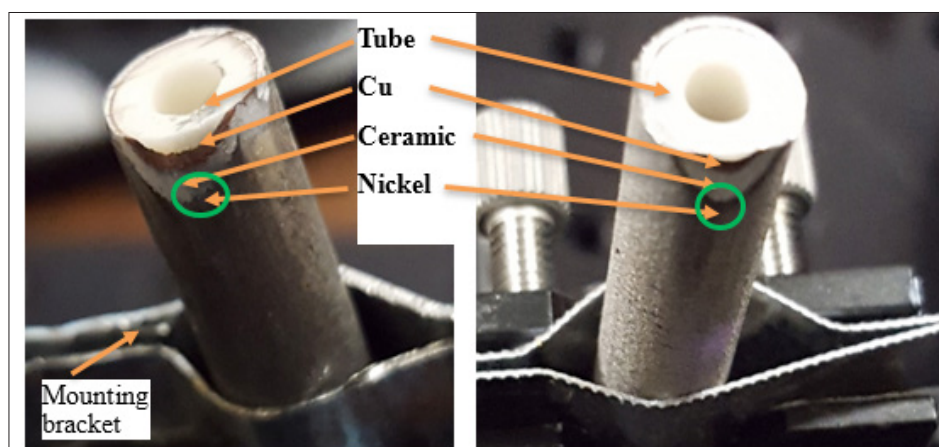

Figure 5: Optical micrograph (left to right) of Sample-77, and Sample-81, after polishing and mounting on the nano scanner. The green circles indicate the interface area of interest for analysis.
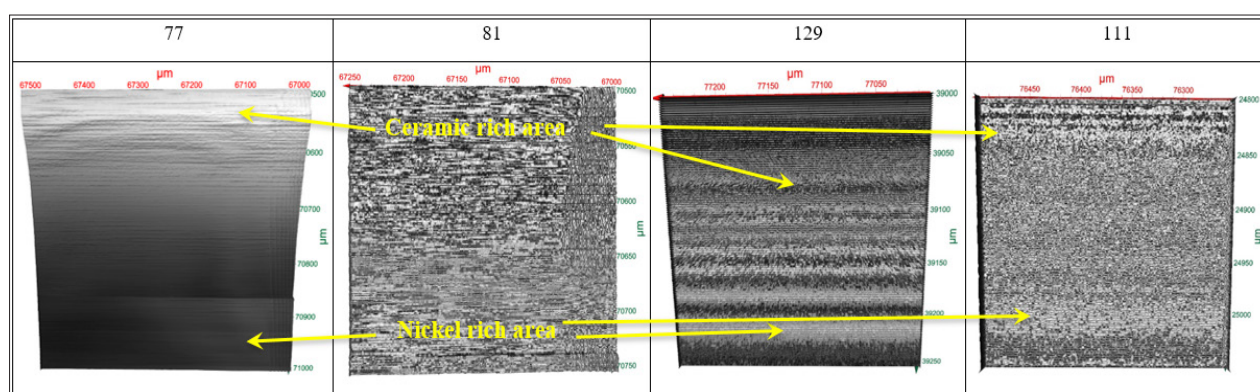
Result

Terahertz image analysis

Figure 6: Close-up image of 4 samples (250µm × 250µm). Low resolution image indicates Nickel rich and ceramic rich areas.

Figure 6 shows a wide area (course) image near the nickel-ceramic interface of the four samples as identified in the header row. The images exhibit surface roughness due to polishing. As indicated on the image, the nickel rich and ceramic rich areas were identified by

1. From the wide area images and

2. From the contrast difference of higher resolution images. Lattice resolution imaging was conducted for each sample on nickel layers near the nickel-ceramic interface.

High resolution imaging results of 4 samples are presented in Figure 7. Embedded nanograins of alumina are visible in all samples. These alumina nanoparticles might get embedded in nickel lattice during the plasma-spray deposition process but may also arise as a side-effect of polishing. Whatever the cause may be, these alumina nanograins caused the lattice deformation of nickel that are visible. Figure 8 shows the high-resolution 3D image of nickel lattice of 4 Samples extracted from Figure 7; each over $(100nm)^3$ volume. Figure 9 exhibit a single surface of the lattice resolution image of all for samples over (100nm × 100nm) each, extracted from Figure 8. A graphical analysis of these lattice images is shown in Figure 10, corresponding to the cursor on each sample in Figure 9. Lattice planes are visible and used for lattice constant measurement from Figure 10 via the standard FWHM method. Table 1 shows the results of measured lattice parameter and calculated unit cell volume, and density. As seen from Table 1, the lattice distance (d) of the 4 samples

of the present investigation is in the order as, $d_{77} < d_{81} < d_{129} < d_{111}$ and higher than the value of metallic nickel. While the sample 77 was not subjected to the aforementioned RF field experiment, yet its lattice parameter is bigger than the metallic nickel. The reason is that the plasma spraying process involve using hydrogen gas in its spraying mechanism; thus, the nickel is already hydrated during deposition which accounts for the lattice dilation. The RF field stress applied during the experiment causes the respective lattice to dilate farther as seen from the data in Table 1.
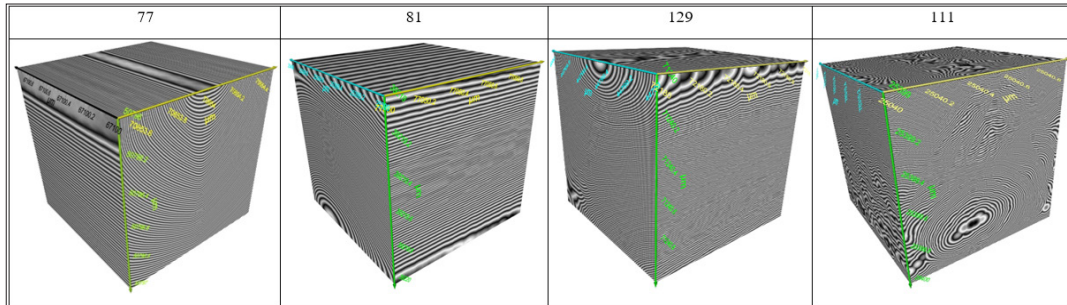

Figure 7: High resolution 3D image of 4 Samples (1µm3) from the Nickel rich area. Embedded nanograins of alumina visible in all samples. These alumina nanograins caused lattice deformation as visible.
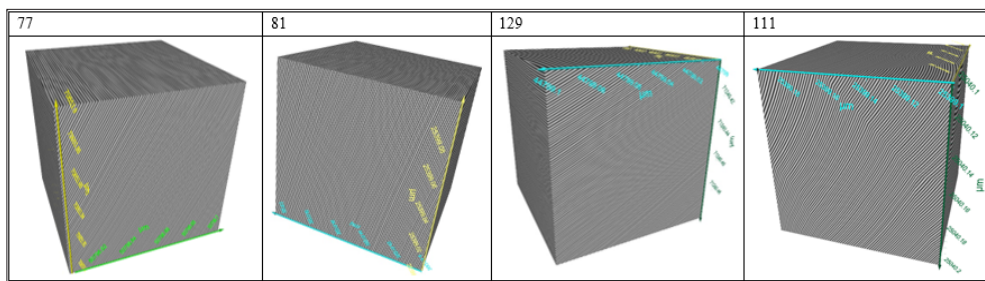
Figure 8: High resolution 3D image of Nickel lattice from 4 Samples (100 nm)3. Lattice plane separation is quantified below.
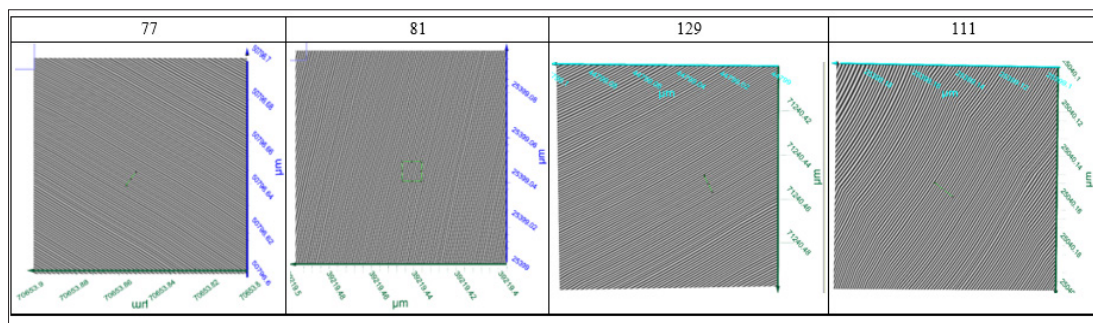
Figure 9: Lattice resolution image of Nickel (100nm × 100nm) extracted for the four samples. Lattice planes are visible and used for lattice constant measurement.

Figure 10: Graphical analysis of the lattice plane corresponding to the cursor for each image in Figure 9. Average lattice plane separation is tabulated in Table 1.

Table 1: Summary of measured lattice parameter and calculated unit cell volume, and density.

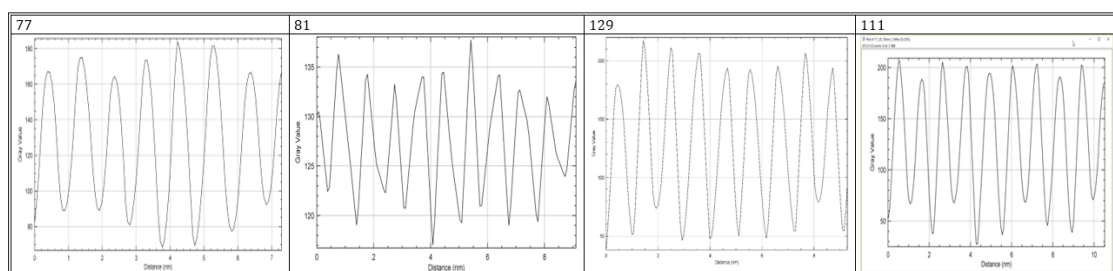| Sample	Metallic nickel	77	81	129	111
Lattice parameter (nm)	0.353	AVERAGE (0.451, 0.448, 0.5, 0.384, 0.448, 0.448) = 0.4465	Av (0.573, 0.446, 0.384, 0.573, 0.445, 0.382, 0.573, 0.573, 0.383) = 0.481	AVERAGE (0.499, 0.436, 0.436, 0.499, 0.499, 0.499, 0.499, 0.498) = 0.483	AVERAGE (0.5, 0.5, 0.5, 0.5, 0.57, 0.5, 0.45) = 0.503
Volume of the Ni unit cell (cm)^3	4.3987×10^{-23}	8.9015×10^{-23}	1.1128×10^{-23}	1.1268×10^{-23}	1.2726×10^{-23}
Density (g/cm^3)	8.863	4.380	3.503	3.460	3.063

*Ni (FCC) has 4 atoms in the unit cell. Molar mass of Ni: 58.6934 g/mol.

$$massofNiUnitcell = \frac{4(58.6934)}{6.022 \times 10^{23}} = 3.8986 \times 10^{-22} g$$

Discussion

The samples of the present investigation (Figure 5) are used for hydrogen gas-based reactors, known as "Hydrogen Hot Tube" (HHT™); see ref. [2] for details. As described in the Experimental section of ref. [2] (pages 1-2), an Iso Peri Bolic Calorimeter ("IPB") is used to measure and validate the energy balance resulting from an HHT reactor experiment. It was summarized that information collected from Brillouin Energy's experimental tests have been corroborated by data checks from independent engineers or physicists demonstrating that its proprietary Q-Pulse™ electronic pulse generator produces excess heat when carefully applied to its engineered nickel core on demand and in repeatable amounts. Excess heat is the amount of thermal energy, which exceeds the original energy used to drive the proprietary Q-Pulse™ electronic pulse generator and its associated electronics [12], proposedly via a mechanism of low energy nuclear reaction or LENR. Therefore, it is customary to make an observation in light of the findings of lattice dilation of the present investigation.

It is further known that the samples 81, 129 and 111 of the present study were subjected to the above mentioned IPB-HHT experiment while sample 77 was not subjected to the HHT experiment, hence serves as a reference. It was also known that samples 81 and 129 produced excess energy supposedly via the LENR process [2] while sample 111, though subjected to the same IPB HHT experiment, did not produce as much output energy as the others. Further, sample 81 produced higher energy than sample 129, with a Coefficients of Performance (COP) of 1.53 for sample 81 while the COP of 1.37 for sample 129. The COP is calculated by dividing the tube's output power gain by the input pulse power [2]. Thus, it is of importance to investigate the lattice scale changes that might have occurred for these samples as a result of being subjected to the IPB-HHT experiments.

Since the LENR process was proposed to be an alternative for the much-discussed cold fusion process [2,3,12- 15], herein we present a brief review of the current status and then try to rationalize the observations by Brillouin Energy [3] in light of the results of the present investigation.

Evaluation of cold fusion

Recently, Berlinguette et al. [13] have revisited the case of cold fusion. The authors re-evaluated cold fusion to a higher standard of scientific rigor. However, despite a rigorous experimental study, they did not find any evidence of such a cold fusion effect. Nonetheless, a by-product of their investigations has been to provide new insights into highly hydrided metals and LENR, and the authors contend that there remains much interesting science to be done in this underexplored parameter space. Though they deployed an entourage of approximately 30 graduate students, postdoctoral researchers and staff scientists since 2015 and conducted numerous experiments; they found that cold fusion has not been proven to exist. Yet they remain convinced to carry out future experiments. The reasons, as stated are,

1. Fusion stands out as a mechanism with enormous potential to affect how we generate energy. This opportunity potential has already mobilized a 25-billion-dollar international investment to construct ITER [14].

2. Evaluating and reevaluating cold fusion led their program to study materials and phenomena that they otherwise might not have considered.

3. Our society is in urgent need of a clean energy breakthrough. Finding breakthroughs requires risk taking, and they contend that revisiting cold fusion is a risk worth taking.

Highly hydrided metals

McKubre and colleagues at SRI International (California, USA) [15] conducted one of the largest studies of cold fusion via Fleischmann-Pons type electrolysis experiments and claimed to observe excess heat only when their palladium cathode was loaded with hydrogen beyond a threshold of PdH$_x$ with x > 0.875, where 'hydrogen' in this perspective represents hydrogen, deuterium,

protons, deuterons, or hydride. The authors determined that understanding how to create, characterize and sustain highly hydrided metals would be a priority. Their cell design enabled the use of X-ray diffraction to measure the loading levels during device operation by tracking the "lattice expansion upon hydrogen absorption."

Is Neutrino the key?

Another important work in this connection was recently reported by Parkhomov [16]. Considering the thermal generation of neutrinos as the basis for nuclear transformations in the LENR process allows the author to explain a number of features of this proposed phenomenon. The author notes that, LENR is very diverse. There are processes in metals with hydrogen dissolved in them that are not quite understood. There are processes in plasma, in a gas discharge, and even in biological systems that need further investigations. At first glance, these processes have nothing in common. But on closer examination, one can see four features that unite them.

1. The first feature is that they have a quite tangible energy threshold (0.1eV)

2. The second feature is that the LENR processes occur in a fairly dense medium (solid, liquid, or dense plasma).

3. The third feature is the large variety of nuclides arising in the LENR process.

4. The fourth feature is the absence (or very low intensity) of hard nuclear radiations (neutrons, gamma quanta), which, it would seem, should inevitably arise during nuclear transmutations.

It has been suggested in the contemporary literature that in order to solve the problem of explaining LENR, it is necessary to involve weak nuclear interactions. Parkhomov [16] tried to show that by taking this path, all the indicated features of LENR can be explained. He further notes that there is no Coulomb barrier in weak interactions (beta-processes). The presence of neutrinos (antineutrinos) is a necessary condition for nuclear transformations to occur due to weak interactions.

Neutrino requires the unavoidable need for a dense environment. The probability of neutrino and antineutrino formation (and hence the cross-section) during thermal collisions of particles of matter is very small. A small probability may be compensated by a large number of collisions but requires a dense medium. Intensive generation (of neutrino and antineutrino) requires a hot, dense medium with a high content of free electrons. In addition to metals, such a medium is a high-density plasma, which briefly arises, for example, during explosions of metallic conductors, or at a sufficiently strong pulsed energy release in liquids. However, neutrinos are considered to be elusive, manifested only in the most complex experiments on huge installations. The properties of neutrinos at very low energies are different from those of "nuclear" neutrinos, because, light differs from gamma radiation, and helium gas differs from alpha particles. The interaction of a huge number of atoms leads to a significant increase in the interaction of neutrinos with matter, resulting in groups of many atoms being involved in nuclear transformations all at once. This, supposedly, could make it possible to explain a number of features of the LENR process.

Comments

So, overall, the current terahertz observation of "lattice dilation" reported in this paper is consistent with the findings of Berlinguette et al. [13] lattice expansion via hydrogen absorption. They make a convincing case for continuing further measurements; thus, further investigation via terahertz imaging and spectroscopy is a likely candidate.

From the circumstantial evidence given in the two papers [13,16] one can reasonably assume that,

1. LENR (if happens) is favored by hydrated metal and other dense medium (also presumably hydrated).

2. The nickel lattice (or palladium), experiences lattice dilation (or "lattice expansion") upon hydrogen absorption at a higher temperature and under an applied AC filed.

3. A decisive mechanism of LENR (if happens) still unknown.

4. In the best possible cases where LENR is suspected, it is still not always reproducible.

Given the above observations, and despite the elaborate investigation reported by Berlinguette et al. [13], there is room for decisive experiments via a "Design of Experiment." The main target is to be able to arrive at a "reproducible" system with predictable behavior. There is no merit of any claim without reproducibility.

Our hypothesis

We hypothesize that the higher energy generation effect observed in the HHT experiments is most likely a "lattice driven phenomenon," as opposed to the nuclear transmutation of some kind or the LENR. So, a systematic investigation, both in-situ and ex-situ, need to be conducted for a conclusive model. A natural question is, where is the increased heat coming from in case of the Brillouin's IPB-HHT experiments [2]? The following hypothesis seems reasonable. It is the "time-crystal like non-equilibrium" process that is driving the energy balance. Time crystals (aka space-time crystal), a newer concept, are states of matter whose patterns repeat at set intervals of time and space. They are systems in which time symmetry is spontaneously broken [17]. A time crystal, thus, is a structure that repeats in time, as well as in space. A time crystal never reaches thermal equilibrium, as it is a type of non-equilibrium matter, a form of matter proposed in 2012 [17].

During the Brillouin IPB-HHT experiment, the tube is heated and then an RF stimulus is applied. The frequency of the RF field is very low, which is in the realm of driving a lattice vibration (potentially, a phonon process). At temperatures high enough, near the glass-transition point, the nickel lattice is rather fluid-like than rigid metal-like. Hence, an applied field will ionize the atoms in their

fluid-like state. The applied thermal energy and an RF filed, either separately or in conjunction, will set the fluid-like nickel lattice in oscillation... Voila! An oscillating ion will undergo non-radiative transition to produce the increased heat energy!

Therefore, an in-situ, time series measurement will pinpoint the correlation between the excess heat and lattice dilation, thus proving or disproving the hypothesis. The basis of the foregoing hypothesis is the well-known electro-optic poling process by which a hyper polarizable material's electro-optic property is modified for higher electro-optic coefficient [18-20]. During the poling process, a material is heated near its glass-transition point and then a high voltage (e.g., 5kV or higher) electric field is applied to "align" the dipoles. The current and temperature are tracked simultaneously to detect the saturation point when all dipoles reach their completely aligned configuration. At that point, the heat is turned off while the field is still being applied; thus, freezing the dipoles in their aligned position. This poled material exhibit a net non-zero second order susceptibility ($\chi^{(2)}$) compared to the unpoled material where the random orientation of the dipoles cancel each other, rendering a net zero dipole moment, and hence zero second order susceptibility. A higher $\chi^{(2)}$ material, when pumped by a suitable laser, becomes a T-ray generator [19].

Thus, it is reasonable to assume that the IPB-HHT experiment creates a similar environment as the poling process; only difference being an applied RF electric field. This key difference is the cause for the above proposed non-radiative process from the lattice vibration at the elevated temperature, where the lattice is expected to be more fluid-like than a rigid covalently bonded hard metal. In this situation, a periodic RF field would most certainly set the lattice atoms in periodic vibration; like a time-crystal; both in time and in space. The observed lattice dilation stipulates the periodic change in the nickel lattice while the observed excess heat stipulates the periodic vibrations.

Therefore, it may be envisioned that the IPB-HHT experiment with the LENR tube cells, when tracked in-situ for its lattice dilation could pinpoint the exact conditions for increased heat energy generation. With this knowledge, one then can refine the LENR tube cell fabrication process for a predictable energy generation process. A simple terahertz setup for tracking the in-situ conditions may be done by means real-time reflection monitoring of the lattice dilation process. This will be investigated as the next project.

Conclusion

The camera-less terahertz imaging technique has been used to investigate the lattice dilation of nickel layer of the LENR tube cell samples. The lattice constant of a metallic nickel was first measured; the value obtained 0.353nm is the same as those accepted value in the literature; thus, verifying the validity of the terahertz imaging technique. Four LENR tube cell samples were subsequently imaged and the nickel lattice constant of each sample was measured following an identical procedure as the metallic nickel. As seen from Table 1, the nickel layer of all LENR tube cell samples have a higher lattice constant compared to the metallic nickel, and consequently

lower density. However, sample 81, 111 and 129 are known to have produced increased heat energy and sample 77 is unused (used as a reference). It was found that the lattice constant (d) of these samples is in the increasing order; i.e., $d_{77} < d_{81} < d_{129} < d_{111}$ and the density is in the decreasing order; i.e., $\rho_{77} > \rho_{81} > \rho_{129} > \rho_{111}$. The density values are 4.380, 3.503, 3.457, and 3.063 for samples 77, 81, 129, and 111, respectively. These are significantly lower than the known density of metallic nickel. To our knowledge, this is the first direct measurement of the lattice dilation phenomenon of plasma-sprayed nickel. The terahertz technique of the present work, thus, proves effective and accurate for lattice imaging, without requiring an electron microscope.

A model has been proposed for explaining the increased heat energy generation from IPB-HHT experiment with the LENR tube cells. Here the fluid-like nickel lattice at higher temperatures, and under the influence of an RF electric field, is assumed to undergo a space-time crystal like non-equilibrium effect; and thus, producing increased energy via a non-radiative transition process. An in-situ monitoring of the IPB-HHT experiment has been proposed to determine the correlation between the excess energy generation period and the observed lattice dilation.

References

1. Rahman A, Rahman AK (2019) Nanoscale metrology of line patterns on semiconductor by continuous wave terahertz multispectral reconstructive 3-d imaging overcoming the abbe diffraction limit. In IEEE Transactions on Semiconductor Manufacturing 32(1): 7-13.

2. https://brillouinenergy.com/newwebsite/wp-content/uploads/2019/04/Brillouin-SRI-Technical-Progress-Report-Final-Public-2018.pdf

3. https://brillouinenergy.com/science-technology

4. Martin ML, Somerday BP, Ritchie RO, Sofronis P (2012) Hydrogen-induced intergranular failure in nickel revisited. Acta Materialia 60: 2739-2745.

5. Anis R, Donald T (2018) Terahertz-based nanometrology: Multispectral imaging of nanoparticles and nanoclusters in suspensions. J Nanopart Res 20: 297.

6. Anis R, Aunik K, William G, Hyeonggon K, Jamal U (2018) Terahertz multispectral imaging for the analysis of gold nanoparticles' size and the number of unit cells in comparison with other techniques. Int J Biosen Bioelectron 4(3): 169-174.

7. Anis R, Aunik K, Yamamoto TY, Kitagawa H (2016) Terahertz sub-nanometer sub-surface imaging of 2D materials. Journal of Biosensors & Bioelectronics 7: 3.

8. Optical Physics. United Kingdom.

9. National Institutes of Health, USA.

10. Han C, Yang S, Chang KG, Wang PP, Song XP, et al. (2015) Structure transition and magnetism of bcc-Ni nanowires. J Mater Chem C 3: 1004-1010.

11. By personal communication with Robert Godes of Brillouinenergy.com.

12. F. Tanzella (2019) Nanosecond pulse stimulation in the ni–h2 system. J Condensed Matter Nucl Sci 29: 202–210.

13. Curtis P, Yet-Ming Chiang, Jeremy N Munday, Thomas Schenkel, David K, et al. (2019) Revisiting the cold case of cold fusion," Nature 570: 45–51.

14. https://www.iter.org/org/team/odg/comm/AnnualReports

15. Michael Mc (2015) Cold fusion: comments on the state of scientific proof. Current Science108(4): 25.

16. http://www.coldreaction.mylittlehomepage.de/module/Download/pdf/Parkhomov-Gutachten.pdf

17. Frank W (2012) Quantum Time Crystals. Physical Review Letters.

18. Blum R, Sprave M, Sablotny J, Eich M (1998) High-electric-field poling of nonlinear optical polymers. J Opt Soc Am B 15: 318-328.

19. Anis R, Aunik R (2012) Wide range broadband terahertz emission from high $\chi^{(2)}$ Dendrimer. In Terahertz Technology and Applications.

20. Anis Rahman, Aunik KR, Donald A (2016) Dendrimer dipole excitation: A new mechanism for terahertz generation. J Biosens Bioelectron 7(1): 196.

For possible submissions Click below:

Submit Article